Spring 5-1-2017

Neurostructural Organization and Neocortical Projecting Neuron Distribution in a Mouse Model of Timothy Syndrome-Mediated Autism Spectrum Disorder

Aiden L. Ford
University of Connecticut - Storrs, aiden.ford@uconn.edu

University of Connecticut

Neurostructural Organization and Neocortical Projecting Neuron Distribution in a Mouse Model of Timothy Syndrome-Mediated Autism Spectrum Disorder

A University Scholar and Honors Thesis submitted in satisfaction of
the requirements for the degree of

Bachelor of Science in Physiology and Neurobiology, Honors
Bachelor of Science in Neurodevelopment and Health, IMJR

Aiden Ford

May 2017

University Scholar Advisory Committee:
Dr. R. Holly Fitch, Chairperson
Dr. Joseph LoTurco
Dr. Inge-Marie Eigsti

Acknowledgements

Thank you. Though simply said, please know that the deepest gratitude and appreciation is built into these words.

I am unbelievably privileged to have had the opportunity to work on this project for the past two and half years. Through it I have grown as a researcher, student, and individual, an impossible evolution without the many people I must thank.

First, my UScholar Committee: Dr. Inge-Marie Eigsti, Dr. Joseph LoTurco, and Dr. Holly Fitch, thank you for guiding and supporting me through the development and execution of this project. Dr. Eigsti, your critical evaluation of how mouse model work engages with human population studies helped me to orient this work within the fields of behavioral and developmental neuroscience and your generous advice has supported me through many questioning moments. Dr. LoTurco, you were a foundational keystone in each step of this project; thank you so much for sharing your lab space and insights. And finally, Dr. Holly Fitch. I remember discovering the lab website back in the spring of my freshman year and immediately knowing it was where I wanted to be. It has been a privilege to learn from such a dynamic and skilled scientist; you are truly an empowering role model. Thank you for helping me open my eyes to the fascinating world of research.

A very special thank you to Amanda Rendall; you are so giving with your expertise and experience. Thank you for letting me be your shadow! To all the past and present graduate students I've been lucky enough to work with, Amanda R., Amanda S. and Peter, thank you! You lead so effortlessly by example.

To my parents, thank you for always asking how the mice were doing and listening to my spiels about perfusions, neurons, and behavioral phenotypes. You were so supportive and encouraging during this project and I am so deeply thankful for all you have given me over the years. And to Liam, I hope I have instilled in you a love for studying mouse neurology, and while I highly doubt my success, thank you regardless for always listening and telling me that my figures looked cool.

My friends, I love you all and am inspired by your creativity, dedication, and determination every single day.

Finally, thank you so much to the many UConn offices who have supported me through this project: the University Scholar program, the Individualized and Interdisciplinary Studies Program, the Office of Undergraduate Research, the IDEA Grant and the Honors Program. Your commitment to championing students as they create the beginnings of their future careers is so instrumental to our successes.

This project was supported by the Summer Undergraduate Research Fellowship, Psychology Undergraduate Research Grant, IDEA Grant, and an NSF IGERT award (PI Magnuson), and by the Murine Behavioral Neurogenetic Facility (MBNF) at the University of Connecticut.

Abstract

Aims: This study investigates the nuanced effect of the *CACNA1C* mutation on neurocognition and neurodevelopment via an extended study of the Timothy Syndrome (TS) mediated Autism Spectrum Disorder (ASD) mouse model – TS2-neo. It includes: (1) an expanded assessment of the TS2-neo behavioral phenotype, and (2) a comprehensive histological analysis of cortical structural and laminar features.

Methods: 24 age-matched male mice – 12 TS2-neo (B6.Cg-Cacna1c^{tm2Itl}, knock-in G406R mutation), 12 WT (C57BL/6J) – were tested on paradigms examining motor, socio-communicative and cognitive abilities. Neural tissue was processed for either volumetric analysis through Nissl stain (8 TS2-neo, 8 WT) or immunohistochemical analysis (4 TS2-neo, 4 WT). Statistics for all analyses were run through SPSS 19.

Results: Analyses of task performance illustrate that TS2-neo mice show impaired sensorimotor and procedural motor learning ability, socio-communicative deficits, increased habitual digging, and strengths in detecting temporal auditory sound cues as compared to WT controls ($p<.05$). Histological analyses of TS2-neo brains reveal significant and marginal decreases in the volumes of the external capsule and fornix ($p<.05$; $p=.059$), aberrant patterns of cortical lamination ($p<.05$), and atypical expression of cortical neuron subpopulations marked by *Satb2* and *Foxp2* ($p<.1$).

Discussion: In this paper we replicate and extend the "ASD-like" behavioral phenotype of the TS2-neo mouse model and report novel findings of atypical white matter development and cortical laminar anomalies in the relative thickness of input and output layers and distribution of markers for projecting neuron populations. These results shed light on possible shifts in global cortico-cortical and cortico-sub-cortical connections in TS-mediated ASD.

Introduction

The autism spectrum disorders (ASDs) encompass a heterogeneous group of neurodevelopmental pathologies defined by an established dyad of observable behavioral symptomology that includes: 1) deficits in the social use of verbal and non-verbal communication; and 2) the persistence of restricted, repetitive actions and interests (American Psychiatric Association, 2013). Current epidemiological estimates predict a prevalence of approximately 1 in 68 in US children with an increasing incidence rate. Lacking a known causative agent/mechanism, research into the genetic etiology of ASD has intensified in the last three decades, and over 150 risk genes have been reliably identified. The subset of ASD cases attributed to a known genetic mutation is classified as syndromic (most notably Fragile-X, Rett's, and Tuberous Sclerosis), however the majority of ASD diagnoses presumably result from as-yet undetermined multifactorial interactions between risk gene mutations and/or environmental risk factors. Transgenic mouse models provide a key research tool for studying the behavioral and anatomical effects of mutations in identified target genes, and have been used to provide clinical insights to the etiology of ASD.

Timothy Syndrome (TS) represents an extremely rare autosomal dominant genetic disorder caused by a *de novo* mutation to the 8A exon of the *CACNA1C* gene, and is one of the established syndromic causes of ASD. Identified in 2004 by a team led by Igor Splawski at Harvard Medical School, approximately 80% of TS cases are accompanied by a co-morbid ASD diagnosis (Splawski et al. 2004). The *CACNA1C* gene encodes a protein integral to the CaV1.2 voltage-gated calcium channel expressed on the surface of neurons and muscle cells (Navedo et al. 2010). The TS-associated mutation prevents the channel from inactivating normally, leading to an overflow of positively charged calcium ions into cells. This particularly affects neurons, which depend on pre-synaptic calcium influx for neurotransmitter release. Implications of this type of developmental abnormality in neural transmission and circuitry are highly relevant to the etiology of ASD.

A knock-in mouse model of TS was developed in 2011, and findings show that the homologous murine mutation (termed "TS2-neo") is associated with a characteristic "ASD-like" phenotype that includes altered social behavior, reduced vocalizations, and perseverative behaviors (Bader et al. 2011). Given the limited literature exploring the TS2-neo mouse model, we designed an expanded behavioral study to elucidate additional behavioral phenotypes associated with the *CACNA1C* mutation in mice.

In addition to serving as a platform for behavioral analysis, mouse models provide an investigative opportunity to examine neurobiological and neurophysiological impacts of ASD-associated risk mutations, with the aim of better understanding neural mechanisms of the disorder. A histological study of the TS2-neo model reported that mutant brains were similar in terms of gross brain shape and weight to wild types, and did not show evidence of gross structural anomalies (Bett et al. 2012). The authors also reported that affected brains were significantly more asymmetric, showed an increased midline angle, and that lateral ventricle cross-section area was also significantly larger in TS2-neo mice. These findings led the research team to conclude that effects of the TS2-neo mutation were subtle, with the majority of changes manifesting in microscopic organization and cellular function (Bett et al., 2012). No studies of which we are aware have explored specific grey and white matter structural volumes and neuronal subpopulation distribution in this model.

Studies using induced pluripotent stem cells (iPSCs) from individuals with Timothy Syndrome have also explored hypotheses regarding altered neuronal function in ASD. For example, in the early stages of cortical neuron differentiation, TS-derived iPSCs were found to exhibit decreased expression of *Satb2*, a biomarker that identifies distant cortical projecting neurons and functionally regulates cortical lamination patterns (Pasca et al. 2011). TS-derived IPSCs also showed an increased expression of *Ctip2*, a biomarker that defines subcortical projecting neurons connecting layer 5 of the cortex and lower structures (midbrain, hindbrain, and spinal cord; Pasca et al. 2011).

The same team replicated decreases in *Satb2* expression in a juvenile conditional mouse model with *CACNA1C* channel mutations restricted to the forebrain. Studies of subcortical biomarker expression have not been conducted in adult TS2-neo mice, which to date represents the only confirmed model of TS-mediated autism. Such studies would be important, given human neuroanatomical ASD studies that report microstructural changes involving persistent developmental alterations in white matter structures (Billeci et al. 2012), including long-range white matter tracts connecting the frontal lobe and limbic system (Amaral et al. 2008, Ameis et al. 2015). Since ASD has been termed a "disconnection syndrome" based on consistent patterns of cortico-cortical hypoconnection, we believe these features should be examined in a TS2-neo mouse model (Melillo et al. 2009).

In addition, a second TS-derived iPSC study published in 2013 found that the TS mutation results in atypical dendritic retraction, including a decrease in the arborization (the length and breadth of dendrites) and complexity of pyramidal neurons from cortex layers 2 and 3 (Krey et al. 2013). These findings were reported in a juvenile TS2-neo mouse model. Assuming this pattern continues into adulthood, we hypothesize that atypical dendritic arbor could impact neocortical lamination and organization. Neocortical lamination is also an important indicator of neuronal connectivity and function. Organized in six distinct layers numbered inward from the molecular (superficial) layer 1 to the deepest (ventricular) layer 6, each layer exhibits a highly consistent pattern of input and output targets determined by signaling from morphological factors in fetal development. Layers 2 and 3, for example, receive information from and project to other cortical regions, while layer 4 is the primary target for incoming sensory projections from the thalamus. Layers 5 and 6, conversely, are projecting layers that send descending output to thalamus (6), and other subcortical structures (5). Cortical regions with specific functions (i.e. motor, auditory, etc.) show further variations in the thickness and complexity of layers with corresponding functionality.

For example, motor regions typically exhibit higher neuronal density/increased thickness in layers 5/6, while primary sensory cortices (A1, V1, S1) show a thicker layer 4.

The current study sought to contribute to the established body of work on the TS2-neo mouse model of TS-mediated ASD by further delving into the nuanced effect of the *CACNA1C* mutation on neurocognition and neurodevelopment. We therefore performed an extended study of the TS2-neo mouse model, with two components: (1) an expanded assessment of the TS2-neo behavioral phenotype, and (2) a quantitative and immunohistochemical analysis of cortical laminar features. Results were expected to provide key insights to the underpinnings of ASD as a neurodevelopmental disorder.

Aims and Hypotheses

Part 1: Behavioral Phenotyping. The primary objective of this portion of the current study was to expand the behavioral phenotype of the TS2-neo mouse model to provide additional validation for this mutant as a model for ASD. We hypothesized, based on published literature, that the TS2-neo mouse would exhibit "ASD-like" behaviors including repetitive behaviors and social/communicative deficits that have already been reported, as well as additional ASD-like patterns of behavior on tasks that have not previously been assessed in this model (reference summary of hypothesized results for specific paradigms in Table 2).

Part 2: Neuroanatomical analysis of structural volume and cortical organization. This portion of the study aimed to explore neuroanatomical differences associated with the *CACNA1C* mutation in Timothy Syndrome (TS), and TS-mediated Autism Spectrum Disorder (ASD) using the TS2-neo mouse model. Specific attention was paid to the volume of critical white matter structures, and the organization of cortical and sub-cortical projecting neuron sub-populations (ascertained by laminar analyses and biomarker expression). We predicted, based on published literature, that we

would observe a decrease in white matter tract volume, as well as atypical distributions of projecting neuron populations.

Methods

Subjects. Two separate cohorts of twelve age-matched (within-cohort) male mice (6 TS2-neo, 6 wild type (WT) (C57BL/6J)) were received from The Jackson Laboratory for a total sample of n=24, (12 TS2-neo, 12 WT). The TS2-neo knock-in mutant (B6.Cg-Cacna1c^{tm2Itl}) included the G406R mutation and an inverted neomycin resistance cassette inserted at the end of exon 8 of the *CACNA1C* gene. The G406R mutation is attributed to severe TS (also called TS2; for additional details on the engineering of the model see Bader et al. 2011). Subjects were single housed on receipt in standard mouse tubs in the Bousfield vivarium, and were provided with a 12h/12h light/dark cycle as well as food and water *ad libitum*. Behavioral testing commenced when animals were adults (postnatal days (P)55-57), well before any age-related sensory loss (Henry & Chole 1980). Testing was conducted blind to genotype and in compliance with the NIH Guide to the Use of Animals in Research, as well as UConn Institute for Animal Care and Use approvals. The behavioral assessments performed included 15 paradigms that tapped motor, social and cognitive ability. Testing was following by sacrifice under anesthesia and perfusion, followed by either standard histology/nissl staining and gross morphometry, or immunohistochemical analyses of select laminar biomarkers.

Rotarod, P57. The Rotarod task assesses sensorimotor ability and procedural motor learning. During the two-minute test trial subjects were placed on a rotating cylinder that accelerated from 4 to 40 rpms. Subjects underwent four individual trials a day, for 5 consecutive days. The dependent measure was latency to fall from the cylinder, with latency values for each trial averaged

for every day/subject. Testing included an initial habituation day (cylinder held at constant speed of 4rpms).

Auditory Processing, P70. All five of the auditory processing tests outlined here are based on a modified pre-pulse inhibition paradigm (PPI; described in Fitch et al. 2008). In brief, PPI measures the acoustic startle reflex (ASR) generated in response to a loud white noise burst (called the startle-eliciting stimulus or SES; 105dB, 50ms, broadband (1-10kHz)). The ASR is a reflexive reaction to this unexpected, intense auditory stimulus. In our paradigm, subjects were placed on individual load-cell platforms programmed to transduce fluctuations in an applied force to a measurable electrical output. Subjects were exposed to an auditory stimulus sequence with a pseudorandom order of cued (burst preceded by a test specific auditory cue) and uncued trials. The ability to detect this cue resulted in a subsequent decrease in the ASR, or "attenuation." The difference in measured ASR for cued vs. uncued trials provided a measure of cue detection, called the attenuation score. This measure derives from the average ASR amplitudes between the cued vs. uncued trials ([average cued ASR/average uncued ASR]*100). Tasks were administered for five days, 300 trials a day, except Normal Single Tone; differences specified below.

Normal Single Tone, P70. Initial testing on Normal Single Tone (NST) determined subjects' baseline auditory ability and pre-pulse inhibition response. NST functions as a control assessment of possible paradigm confounds, including general auditory ability and gross motor reflexes. Sessions involved 104 trials, pseudo-randomly ordered as cued or uncued with inter-trial intervals of varying length (16-24s). Stimulus background was silent and the auditory cue was a simple single tone at 8,000 Hz (75dB). This task was administered for 1 day. All subjects showed significant and comparable detection of the cue, and therefore were advanced to further auditory processing tasks.

Embedded Tone, P71. The Embedded Tone (EBT) paradigm assesses ability to detect changes in tone duration relative to an unchanging background tone. The variable cue was a 5.6kHz

pure tone within the 10.5kHz pure background tone. Subjects underwent 2 EBT sessions: the first with long duration cues (0-100ms) and the second with short duration cues (0-10ms) presented before the noise burst. Each session lasted five consecutive days. Uncued trials used a tone duration of 0ms. Pairing the EBT tasks (long and short) allowed for the determination of genotype-specific detection thresholds because the second paradigm, which is more difficult, challenges the possibility of comparable performances between groups on the first task.

Silent Gap, P86. Silent Gap is designed to assess the ability to detect sound breaks in continuous white noise (75dB broadband background). Trials were pseudorandomly cued and uncued. Two 5-day sessions of Silent Gap were conducted, the first with long duration gaps (0-100ms) and the second with short duration gaps (0-10ms). A gap duration of 0 ms was used for uncued trials in both sessions. As in EBT, the dual sessions allow for a more nuanced determination of ceiling and basement detection values and experimental group-specific detection thresholds.

Pitch Discrimination, P101. Pitch Discrimination assesses subject ability to detect minute variations in the pitch of a 300ms tone cue embedded in a standard background tone (75 dB, 10,500Hz). The cue tone varied from the background by 5-75Hz and was played after a variable inter-trial interval (16-24s). Uncued trials had no deviations in pitch.

Social Dominance Tube Test, P113. To assess dominance and aggression in social contexts, subjects competed for space in a hollow plexiglass tube. A randomly selected pairing of WT and mutant subjects was placed one on either side of the tube and released into it together. The tube's narrow diameter prevented the mice from turning around, so the first mouse to back out was deemed the "loser" with other the "trial winner." Every mouse underwent 4 trials, each with a new random pair subject (never a same-genotype match), and their percentage of trial wins was calculated for analysis. All subjects were habituated to the tube environment prior to testing.

Marble burying, P115. To assess repetitive digging behaviors, subjects were placed in a standard large rodent cage filled with fresh bedding at a depth of approximately 2 inches. Glass toy marbles were evenly distributed across the bedding in 3 rows of 7. Subjects were allowed to freely roam around the cage for 45 minutes; the number of marbles buried was counted as the outcome variable, "buried" criterion was 2/3 covered in bedding.

Ultrasonic Vocalizations, P122. Adult subjects were recorded for five minutes during male-female pair social interactions to assess emitted vocal response to the presence of a female and female urinary estrus hormones. Subjects were age-matched with a WT C57 female and male-female pairs were placed in a standard mouse cage with seven-day old bedding obtained from the same female. All vocal emissions were recorded using a 1/4inch condenser microphone hanging 10cm above the testing environment, and recorded sound waveforms were analyzed using *Adobe Audition*. The outcome measure was total time spent vocalizing, as calculated by delineating periods of continuous vocalizations from periods of silence. Time vocalizing was binned into minute blocks across the five-minute testing period.

Water Escape, P127. Prior to all water-based cognitive testing, subjects underwent an escape test to assess general swimming ability, with no differences observed between groups. In this task, subjects were placed on one end of a narrow oval tub and given 45 seconds to swim to a visible escape platform at the other end. Latency to reach the platform was recorded.

Morris Water Maze, P129. The Morris Water Maze (MWM) is a standard behavioral assessment for spatial learning and memory. Subjects are required to use room cues to locate a submerged escape platform; latency to find this platform is measured as the outcome variable. Testing occurred over five consecutive days; each subject had one testing session of four trials per day. During each trial, the subject was placed at the starting location, one of the four compass points, north, south, east, and west. The order of the starting location was randomly selected and

used only once over the course of the day's testing session. Therefore, the location of the target platform remained the same over the course of testing in relation to extra-maze room cues and subjects were expected to use those cues to orient themselves to its location after random placement at different start points. Trials timed out after 45 seconds, at which the unsuccessful subject was gently led to the platform before being removed. Subject performance was recorded using a video-tracking program.

4/8 Radial Arm Maze, P136. After the MWM, subjects proceeded to a water adaption of the 4/8 radial arm maze (Hyde, Hoplight & Denenberg, 1998). This task is used to simultaneously assess spatial learning, as well as reference and working memory ability. In this task, four of the eight available entry arms were targets and held a submerged goal platform, while the other four were empty. All entry arms were open during testing. During this task, subjects again used extra-maze cues to orient themselves to target locations. Goal arm selection was fixed per subject and counterbalanced between subjects.

Task training occurred on Day 1, right before the start of testing. During this period, all non-target arms were blocked, which forced subjects to only enter and familiarize themselves with the entry arms containing goal platforms. Subjects were given 120 seconds to locate a platform after start time. If unsuccessful, they were gently guided to the nearest platform. Once on the platform, subjects remained for 20 seconds and then were removed from the maze to their home cage (30 second inter-trial interval; ITI). After each of the four trials, the identified target arm was blocked and the platform removed, ensuring that subjects would have to locate all of the four target arms.

The testing period began on Day 2 and lasted for 15 consecutive days. Over the course of four 120-second trials per day, animals were required to enter all four target arms (one per trial) and locate the accompanying submerged goal platforms (or be guided to the nearest if unsuccessful). At the end of each trial, the identified goal platform was removed, but the target arm remained open

and available for entry (although lacking the means to gain the task reward of removal from the water). Therefore, the task required subjects to: (a) locate target arms using extra-maze cues; (b) remember the specific 4 target arms; and (c) remember which arms they had already entered during that testing session. Subject performance was again recorded using a video-tracking program. Latency and path distance were outcome variables, and the number of reference and working memory errors were recorded for analysis.

Statistical Analyses, Behavior. Results from all 24 subjects (Ts2-neo 12, WT 12) were used for behavioral analyses. All analyses were conducted using SPSS 19, with a significance criterion of 0.05 (two-tailed). For the Rotarod task, subject group differences were measured using a 2 (Genotype) * 5(day) repeated measures analysis of variance (ANOVA). Statistical analyses were conducted on EBT, Silent Gap and Pitch Discrimination paradigms using subject NST score as a covariate. Differences in attenuation scores across these paradigms were examined using a 2 (Genotype) * 5 (Day) * 9 (number of cue levels) repeated measures ANOVA. The social dominance tube test, marble burying, ultrasonic vocalizations, and water escape paradigms were all assessed via univariate ANOVA to assess Genotype effects. Performance on the Morris Water Maze and 4/8 Radial arm maze were analyzed using repeated measures ANOVA. For the MWM, a 2 (Genotype) * 5 (Day) test was used to assess group differences in latency, and average total errors for the 4/8 were analyzed via 2 (Genotype) * 14 (Day) ANOVA.

Perfusion and histology, P191. At the completion of testing, all 24 subjects were weighed, anesthetized using ketamine (100mg/kg) and xylazine (15 mg/kg), and transcardially perfused using a .09% saline solution with formalin as the fixative. Brains were extracted and stored in formalin to postfix at 4°C. Sixteen tissue samples (8 TS2-neo, 8 WT) were stored long-term to await volumetric assessment of neuroanatomy using Nissl stain. The remaining 8 subject samples (4 TS2-neo, 4 WT) were dehydrated in ethanol within 24 hours after initial formalin immersion and embedded in

paraffin wax, following established processing protocols. Once embedded, they were stored at room temperature to await slicing and immunohistochemical staining.

Nissl staining and stereology. Formalin-fixed brains were serially sectioned in the coronal plane at 60 μm using a vibratome. Every second section was mounted on gelatin-subbed slides and stained for Nissl bodies using cresyl violet (coverslipped with DPX mounting medium). Volumes of grey matter and white matter structures were assessed. Select cortical structures included the motor, sensorimotor, and auditory cortices. White matter structures included corpus callosum, cingulum, external and internal capsule, fornix, and anterior commissure. For all structures, volumes were evaluated using the Cavalieri Estimator probe in *StereoInvesigator* together with a Zeiss Axio Imager A2 microscope. Average numbers of sections analyzed per structure are shown in Table 1. A standard stereotaxic atlas was used to determine structure borders (Lein et al. 2007). We also collected measures of cortical laminar thickness in the motor cortex at Bregma levels 1.10, .14, and -1.14 to assess atypical cortical organization in the TS2-neo mutant. The cortex was divided into an upper layer region (layers 2-4) and a deep layer region (layers 5 and 6) using the same standard stereotaxic atlas. All measurements were performed blind to Genotype.

Immunohistochemistry (IHC). Immunohistochemical analysis was used to label cortical neuron subpopulations identified by *Satb2*, *Ctip2*, and *Foxp2* biomarkers. Paraffin embedded tissue was mounted on a microtome and coronal sections (5μm) from bregma -2.00 were prepared for staining. Sections were de-paraffinized, permeabilized, blocked, and incubated at 23°C for 60 minutes with the following antibodies: *Satb2* specific antibody raised in mouse, *Ctip2* specific antibody raised in rat, and *Foxp2* specific antibody raised in rat. Samples were then washed using TBS at 23°C and incubated for 1 hour with biotinylated secondary antibody to be viewed by the ABC method with diaminobenzidine (DAB). Slides were coverslipped-using DPX mounting medium and imaged using *StereoInvesigator* together with a Zeiss Axio Imager A2 microscope. All

measurements were performed blind to Genotype. Target cortical regions – motor, somatosensory, auditory – were outlined and stained cells were counted (x per mm^2).

Statistical Analyses, neuromorphology. Subjects in each of the two *post mortem* tissue groups -- Nissl stained (n=16, 8 TS2-neo/8 WT)) and IHC (n=8, 4 TS2-neo/4 WT)) -- were used for analysis. Group differences in volume region and cortical thickness were assessed using a univariate ANOVA. Group differences in mean number of cells per mm^2 in each of the targeted cortical regions were analyzed via univariate ANOVA. Further analyses were completed using repeated measures ANOVA (Region*Genotype). All analyses were conducted using SPSS 19 with a significance criterion of 0.05, two-tailed.

Results

Rotarod: TS2neo mice show impairments in sensorimotor ability and procedural motor learning. Analyses of mean latency to fall showed a main effect of Genotype [$F(1,22)=14.037$, $p<.05$], as well as a Genotype*Day interaction [$F(1,22)=8.251$, $p<.001$]. Specifically, TS2-neo mutants had a significantly shorter latency to fall than WTs, evidencing sensorimotor deficits (seen in Figure 1A). Moreover, Ts2-neo mice showed a lack of improvement over the course of testing, indicating impairments in procedural motor learning.

Auditory processing: TS2-neo knock-ins performed significantly better on more difficult embedded tone and silent gap auditory processing paradigms. Preliminary analyses of NST results revealed no main effect of Genotype, thus excluding confounds due to auditory or gross motor impairments. To control for individual variation in baseline performance, all further auditory analyses were conducted using NST as a covariate.

Analysis of the first session of embedded tone testing (0-100ms) revealed no significant differences between groups [$p>.05$]. The second session of EBT (0-10ms), which is the more

difficult paradigm because stimuli are much shorter, revealed a main Genotype effect [$F(1,22)=1.394$, $p<.05$] (seen in Figure 1B). Specifically, TS2-neo mice were significantly *better* at detecting shorter embedded tone cues than WTs. Similar results were seen on the Silent Gap task. Specifically, assessment of the basic round of silent gap testing (cues lasting 0-300ms) revealed no main effect of Genotype, but analysis of the subsequent 0-100ms silent gap task again showed a Genotype effect [$F(1,22)=7.369$, $p<.05$] with the TS2-neo group performing significantly *better* than the WTs (seen in Figure 1C). Analysis of the pitch discrimination task revealed no main effect of Genotype [$p>.05$].

Tube-task & vocalizations: TS2-neo mice display significantly atypical interactive social behaviors. Analysis of the social dominance tube test compared "number of wins," which revealed a main effect of Genotype [$F(1,22)=12.138$, $p<.01$]. Specifically, the TS2-neo mice "won" significantly more trials than WT controls, indicating that TS2-neo mice were more socially aggressive (Figure 1). Analysis of ultrasonic vocalizations, which assessed time spent vocalizing (s) per each minute of interaction with the female as a function of Genotype, showed that the TS2-neo mice vocalized significantly *less* after the initial two minutes of the interaction (seen in Figure 1E), [Minute 1: $F(1,22)=.187$, $p>.05$; Minute 2: $F(1,22)=.180$, $p>.05$; Minute 3: $F(1,22)=4.803$, $p<.05$; Minute 4: $F(1,22)=.4.058$, $p<.10$; Minute 5: $F(1,22)=6.498$, $p<.05$]. Again this indicated atypical social behavior for the TS2-neo group.

Marble-burying: TS2-neo mice bury significantly more marbles. Analysis revealed a main effect of Genotype on the marble-burying task [$F(1,22)=10.662$, $p<.01$], with TS2-neo mice burying significantly *more* marbles compared to WTs. This indicates perseverative expression of stereotypical digging behaviors in this model (seen in Figure 1D).

Water maze tasks: Assessment of memory and learning shows no impairments in TS2-neo model. Analysis of water escape performance using univariate ANOVA revealed no

significant differences between subject groups, indicating no confounds in motor or visual ability for further analysis of the MWM and 4/8 Radial Arm Maze.

Analysis of the MWM showed a main effect of Day [$F(1,22)=6.313$, $p<.01$], but not Genotype [$p>.05$]. This indicates that both groups had significantly decreased latencies over the course of testing, meaning that all subjects were able to effectively learn and complete this task. Analysis of performance on the radial arm maze further delineated specific types of errors made, including working memory, initial reference, and repeated reference errors. A repeated measures ANOVA on the average number of total errors revealed no significant effect of Genotype [$p>.05$], but did show a main effect of Day [$F(1,22)=5.348$, $p<.01$]. This indicates that both groups learned the task (i.e., reduced errors made over the course of testing). More in-depth individual analyses of the error types also showed no main effects of Genotype [$p>.05$].

Summary of results from *Part 1: Behavioral Phenotyping* seen in Table 2.

Neuroanatomic volumes: Evidence of decreased external capsule and fornix (white matter) volume in TS2-neo mouse model. Initial analysis of white matter tract volumes (Nissl stained samples, n=16 (8 Ts2-neo/8 WT)), revealed a main effect of Genotype on volume of external capsule volume between groups. Specifically, TS2-neo mice show a significantly *smaller* external capsule volume compared to WT controls [$F(1,16)=6.417$, $p<.05$] (seen Figure 2A,B). A subsequent examination of hemisphere-dependent effects showed that the significant decrease was localized to the right external capsule [$F(1,16)=10.737$ $p<.01$]. Analysis of total fornix volume also showed a trend towards reduced volume in the TS2-neo group [$F(1,16)=4.209$, $p<.1$] (seen Figure 2A,C). No Genotype differences were seen for other white matter structures assessed.

Volumes of targeted grey matter cortical structures – motor cortex, sensorimotor cortex, and auditory cortex – were also examined, both for total volume and then right and left hemisphere

volumes. Examination of all grey matter structure volumes revealed no significant differences in size between Genotypes.

Immunohistochemistry: TS2-neo mice show a shift towards a decreased population of neurons expressing Satb2. Results of immunohistochemical staining (n=8 (4 Ts2-neo/4 WT)) for *Satb2, Ctip2*, and *Foxp2*-expressing cortical neuron subpopulations were evaluated as total counts, counts by target cortical region (motor cortex, somatosensory cortex, and auditory cortex), and by left-right hemisphere target regions. Analysis of *Satb2* expressing cells showed a trending effect of Genotype, with a decrease in this cortical neuron sub-population in the left somatosensory cortex of the TS2-neo population [$F(1,4)=.010$, $p<.1$]. An overall pattern of decreased *Satb2* expression was also seen in the TS2-neo cortex (seen in Figure 3A-C). Repeated measures ANOVA of expression in target regions across the left hemisphere indicated a supporting trend towards a significant reduction in *Satb2* expression specifically in the somatosensory cortex [$F(1,4)=4.346$, $p<.1$]. Examination of the *Foxp2* subpopulation revealed a trend towards a significant increase of these cells in the left motor cortex of the TS2-neo model [$F(1,4)=3.521$, $p<.1$] (Figure 4A-C). No main effect of Genotype was observed in *Ctip2* expression between groups. Notably, the necessary division of the subject pool into two subsets for the volumetric and immunohistochemical experiments resulted in a very small subject pool for the immunohistochemical study (4 TS2-neo, 4 WT). This statistical limitation, in combination with high variance, likely greatly reduced the statistical power of these analyses.

Evidence of increased deep layer thickness and corresponding decreases in upper layers in TS2-neo mutant. Again using the Nissl-stained samples (n=16 (8 Ts2-neo/8 WT)), we analyzed cortical layer thickness (μm) across three Bregma levels of the motor cortex, specifically to look for any neurostructural manifestation of the atypical expression observed for laminar biomarkers *Satb2* and *Foxp2*. Univariate ANOVA revealed no differences in overall cortical

thickness between groups, but a significant pattern of atypical laminar organization in the TS2-neo mutant was observed. Specifically, measures showed a shift towards *increased* deep layer thickness (L5 and L6), as well as corresponding *decreases* in the upper neocortical layers (L 2-4) in TS2-neo mice. Results further showed a particularly significant effect in the left hemisphere (Table 3, Figure 5A-C).

Discussion

The current study used a TS2-neo mouse model of the *CACNA1C* mutation associated with both Timothy Syndrome (and secondarily, ASD) to replicate and extend an "ASD-like" behavioral phenotype. In addition, we report new evidence of atypical white matter development, also consistent with the existing body of ASD mouse model and human research. Finally, we report cortical laminar anomalies -- both in relative thickness of input and output layers, as well as atypical distribution of markers for projecting neuron populations -- shedding light on possible shifts in global cortico-cortical and cortico-sub-cortical connections in ASD.

Expanded Behavioral Phenotype and validation of the TS2-neo mutant as a mouse model of ASD. The TS2-neo mouse model exhibits the core symptomology dyad characteristics of ASD, including: (1) repetitive stereotyped behaviors, and; (2) anomalies in social behavior and communication. TS2-neo mice buried nearly twice as many marbles as their WT counterparts over the course of the 45-minute testing period, a measure of pronounced stereotypical digging behavior. Bader et al. (2011) reported nearly identical results, and collectively these findings strongly validate the presence of persistent "ASD-like" repetitive stereotypical behaviors in this model. In addition, results from two socio-communicative paradigms -- ultrasonic vocalizations, and the social dominance tube task -- revealed impairments in typical social interaction, again affirming an "ASD-like" profile in the TS2-neo model. Specifically, early and persistent abnormalities in reciprocal social behavior are standard markers of an ASD diagnosis in humans, and atypicalities in representative

mouse social settings provide a powerful paradigm to assess social development in mouse ASD models (Scattoni et al. 2008). We saw that over the course of a five-minute male-female interaction, male mutants communicated significantly less in the last three minutes, vocalizing only half as much as WT controls during that period. TS2-neo mice also show shorter alarm calls in response to separation from their mothers (Bader et al. 2011), suggesting that this model shows consistent communication anomalies through the lifespan. Secondly, we assessed social cognition (dominance and aggression) via the Tube Test. Anomalies in the number of "wins" when competing for space (indicating either increased or decreased social dominance) have been reported in ASD mouse models, although both increases and decreases have been observed depending on the model (Kazdoba et al. 2016). We found that TS2-neo mice were significantly more likely to "win" the territory competition for tube space. However, rather than forcefully push the opposing mouse out of the tube, observations showed that the TS2-neo mice tended to freeze in place and completely disengage from social engagement initiated by their WT pair. This behavior may relate to a similar withdrawal during the mating interaction as shown by the decrease in vocalizations, again indicating an atypical pattern of social behavior in this model.

Results from the rapid auditory processing and memory and learning assays further expand this behavioral phenotype. TS2-neo mice showed very little improvement on the Rotarod task over the course of the five days of testing, indicative of impairments in motor coordination and procedural learning. These deficits in fundamental motor abilities may underlie other patterns of atypical neurocognition in ASD and suggest hypo-connectivity of long-range white matter frontal-cerebellar and frontal-striatal tracts (Mostofsky et al. 2000, Mostofsky et al. 2009). Assessment of spatial learning and memory through water-based maze tasks showed no TS2-neo specific deficits in these cognitive domains. Bader et al. examined perseverative behaviors through the Morris Water Maze and found inflexibility to learning new platform locations. Ultimately, TS2-neo mice are

completely capable of mastering tasks of high cognitive load as represented through performance on the 4/8 Radial Maze, but may require more time to re-learn established stimuli and success criteria.

Rapid auditory processing ability is a critical foundation for later language development. Analysis of TS2-neo performance on five pre-pulse inhibition paradigms revealed superiorities on the embedded tone and silent gap tasks. Our lab has found similar superiorities in another established mouse model of ASD, *Cntnap2* (Truong et al. 2015), and this pattern is consistent with the human population, where ASD-related auditory hypersensitivity is extremely common (Gomes et al. 2004) and implicated in deficits in normal language development (Eigsi & Fein, 2013).

Ultimately, our results show that developmental inactivation of voltage-gated CaV1.2 calcium channels (via *CACNAC1* mutation) results in a TS-mediated ASD-like phenotype characterized by impaired social interaction and increased repetitive actions, improved rapid auditory processing ability, and motor-specific procedural learning deficits.

Implications for the enhanced perceptual functioning and cortico-cortical disconnection theories. The behavioral phenotype validated in the TS2-neo mouse model aligns with the enhanced perceptual functioning theory of ASD put forth by Mottron et al. (2006). They contend that the dichotomous pairing of enhanced sensory perceptual abilities and compromised global sensory integration founding characteristic ASD symptomology, in particular socio-communicative deficits, and can be explained by a developmental re-orientation of cortical functional patterns. Locally oriented "low-level" processing mechanisms are enhanced and favored over more complex, integrative strategies that engage global and long-range processing mechanisms. This may manifest neurocognitively as regional hyper-connectivity and long-range hypo-connectivity. Martinez-Sanchis elaborates that this unconscious preference for regional specific integration would ultimately enhance these locally processed low-level sensory perception abilities (2014). Specifically considering the behavioral results on the TS2-neo mouse model, this pattern

emerges as strengths in fundamental processing tasks, i.e. better performance on rapid auditory processing tasks with higher cognitive load, and deficits in social interactions reliant on a multitude of behavioral and communicative cues, i.e. mating or territorial competitions. In the neuroanatomical study discussed next, we explore how this skewed balance between intracortical hypoconnectivity and subcortical hyper connectivity manifests in TS2-neo neuroanatomy.

Atypical white matter development in the TS2-neo mouse model. A growing body of neuroimaging studies identifies abnormal development of white matter tracts and organization of grey matter structures as markers of an ASD neurostructural phenotype, which we saw reflected in our own results. In the current study, we report novel reductions in the volumes of the external capsule and fornix, two major white matter tracts. The external capsule contains cortico-cortical association fibers that form the basis of intercortical communication between the basal forebrain and other regions of the cerebral cortex and the fornix is a bundle of commissural fibers connecting the hippocampus, mammillary bodies, and thalamus between the two hemispheres of the brain. Our findings of reductions in the fornix parallel reported results from neuroanatomical studies of the BTBR and NL3 mouse models of ASD. Ellegood et al. saw decreased fornix volume in both of these models and decreased fornix integrity via a lower fractional anisotropy measure in the BTBR mouse (2015). Collectively, these results contribute to the larger body of work assessing ASD as a disorder of hypoconnectivity and disconnection between fronto-cortical and cortico-cortical networks. These pathways are critical for the integration of information that promotes normative socio-communicative development and deficits in connection integrity and structure are correlated with ASD symptom severity (Alexander et al. 2007, Poustka et al. 2012). This pattern of aberrant white matter development in ASD has become so consistent that some suggest that with further research it could become a unifying neuro-endophenotype.

Non-normative expression of biomarkers identifying cortical subpopulations associated with the development of long-range cortico-cortical and subcortical projecting neurons. Results from quantitative analysis of *Satb2*, *Foxp2*, and *Ctip2* biomarker expression in the TS2-neo neocortex support atypical distribution and organization of specific cortical neuron subpopulations. We saw a consistent decrease in *Satb2*-expressing neurons across the specific functional regions of the neocortex (motor, sensorimotor, and auditory), as well as trends towards a significant decrease in the left sensory-motor cortex. This shift is supported by previous work from Pasca et al. (2011) who found a similar decrease in *Satb2* expression in a juvenile conditional knock-in TS mouse model. *Satb2* is also a confirmed ASD risk gene; whole-genome sequencing studies have found a missense mutation associated with ASD diagnosis in identified probands (Jiang et al. 2013).

Decreased *Satb2* expression has important implications for white matter tract and neocortical development because *Satb2* is a post-mitotic determinant of cortical neuron identity (Britanova et al. 2008) A DNA-binding protein necessary for transcriptional regulation and chromatin remodeling, *Satb2*-expressing neurons preferentially migrate to layers 2 and 3 of the neocortex and project through the corpus callosum to connect the left and right hemisphere. Early in fetal development, *Satb2* expression drives the speciation of upper layer neurons (UL). Loss of this transcription factor has severe impacts; *Satb2* knockouts have substantially compromised migration and laminar organization. Specific effects include delayed migration of later born UL neurons and the potential failure to migrate past deep layer neurons (DL), uniting these two subpopulations in the deep layers of the neocortex. Beyond malformed lamination, projecting neurons that typically route through intracortical callosal tracts deviate to subcortical projections in *Satb2* knockouts. Imagine a balance beam: normal Satb2 expression and typical development results in the usual balance between subcortical and cortico-cortical connections, but in the absence of *Satb2*, layer 2 and 3 neurons do

not engage proper speciation mechanisms and preferentially project through subcortical tracts, decreasing the strength and integrity of critical intracortical pathways.

Based on these findings, we can posit that altered *Satb2* neocortical expression in neurodevelopment leads to changes in the altered WMT development and relative thickness of the cortical layers – both of which we found in our neurostructural analysis of the TS2-neo model. Specifically, layers 5 and 6 of the TS2-neo right motor cortex were found to be significantly thicker than layers 2-3. These results are supported by the expression pattern of *Foxp2* neurons. *Foxp2* is a forkhead box protein that drives fetal brain development and preferentially marks deep layer cortical neurons (layers 5 and 6). We saw a nearly significant increase of *Foxp2* neurons in the right motor cortex of the TS2-neo, suggesting a quantitative increase of neurons preferentially located in the deep layers of the neocortex. No significant differences were found in *Ctip2* expression.

Ultimately these findings tie into a cohesive narrative of atypical neural connectivity in the TS2-neo mouse model of ASD. On the molecular level, we see a decrease in *Satb2* expression, which could potentially drive aberrant development of cortical lamination and cortico-cortical projections. We also see these corresponding structural impacts in TS2-neo neuroanatomy: significant increases in deep layer thickness, which form the foundation of subcortical white matter connections, and significant decreases in cortico-cortical white matter tracts. Due to lack of statistical power, we cannot offer further conclusions; only encourage further study of the neurobiological mechanisms that scaffold this abnormal pattern of cortical development.

Future Directions

Confirmation and clarification of these atypical patterns of intracortical connectivity will require a larger-population study to reduce the influence of intra-subject variability and allow for correlational analysis between behavioral and neuroanatomical parameters. Further analysis of the aberrant

laminar patterns of neuron distribution and migration, achieved through co-expressive immunohistochemical techniques, would also allow for a more specific understanding of how the *CACNA1C* mutation impairs speciation and differentiation of upper and lower layer neurons. If paired with an antero and retrograde tracing studies of neuronal projection in the TS2-neo neocortex to confirm origin and target regions of cell subpopulations, we could achieve a highly nuanced understanding of cortical connectivity in this model with implications for existing theories for general connectivity in ASD.

Figures and Tables

Structure	Corpus Callosum	Cingulum	External Capsule	Internal Capsule	Anterior Commissure	Fornix	Somato-sensory Cortex	Motor Cortex	Auditory Cortex
Average number of sections	9.75	8.69	8.81	9.43	9.75	9.59	9.47	9.47	9.17

Table 1: Average number of sections analyzed across all subjects for the volumetric analyses of associated white and grey matter structures using Cavalieri's Estimator.

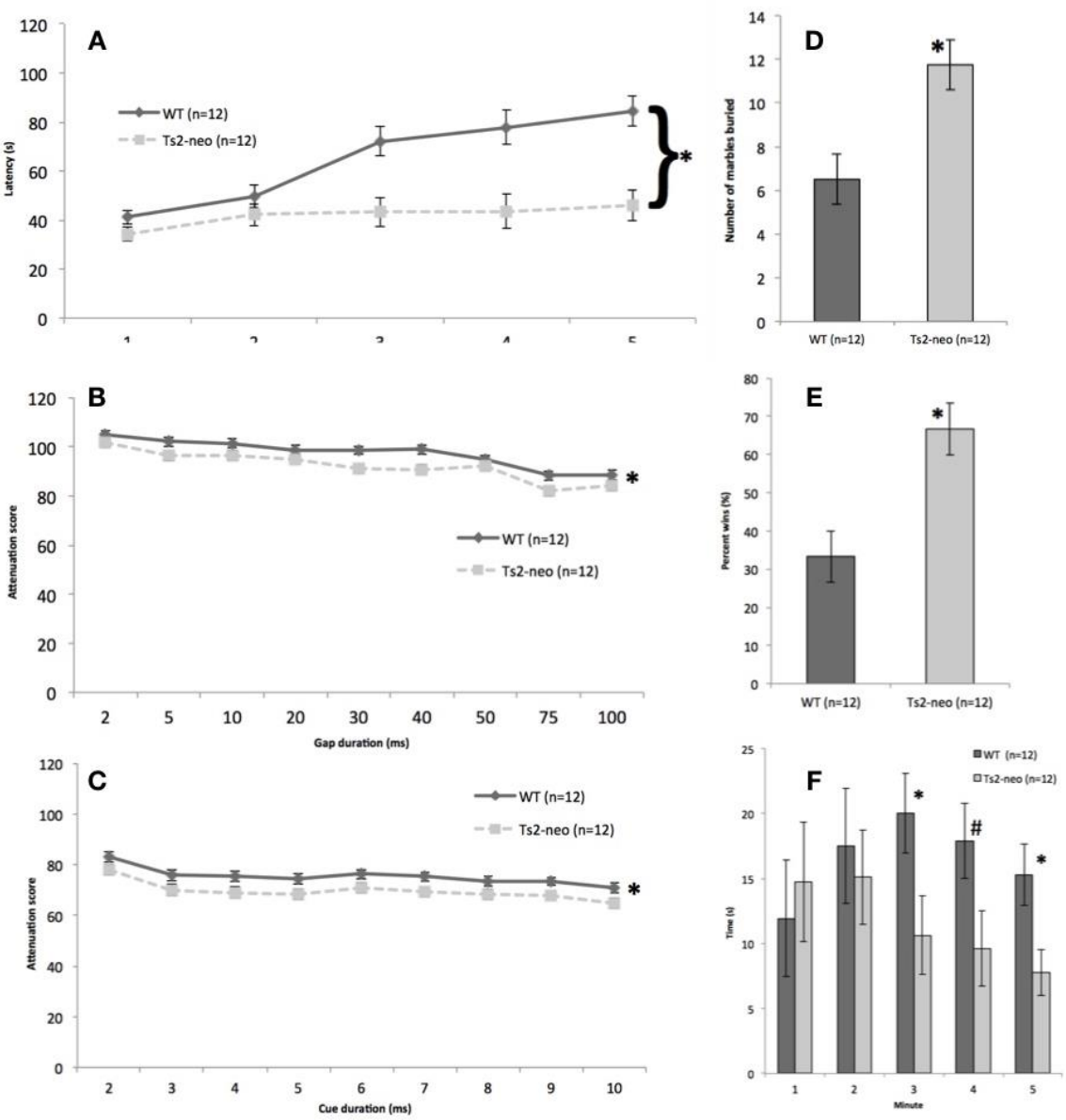

Figure 1: TS2-neo mice display an intermediary ASD-like phenotype with specific behavioral replication of the core symptomology dyad. (A) TS2-neo mice show significant impairments in motor procedural learning; their latency on the Rotarod task is distinctly stagnant over the 5-day testing period. (B, C) TS2-neo mice show enhancements in rapid auditory processing; they are able to distinguish shorter temporal cues in both the embedded tone and silent gap tests as compared to WT controls. (D) TS2-neo mice buried significantly more marbles than WTs, an indicator of habitual digging and burying behaviors. (E) TS2-neo mice were more socially aggressive and "won" significantly more bouts of the space-competition paradigm, the Test Tube Task. (F) TS2-neo male mice vocalized significantly less over the course of a potential mating interaction than WT male controls, particularly in the last three minutes of the interaction.

Task	**Expected Results**	**Reported Results**
Rotarod Task	Impaired performance in the TS2-neo mice. (Motofsky et al. 2000; Moy et al. 2007)	TS2-neo mice show significant deficits in procedural learning and motor ability.
Rapid Auditory Processing Paradigms	Enhancements in paradigm performance of TS2-neo mice. (Truong et al. 2015)	TS2-neo mice were significantly *better* at detecting shorter embedded tone and silent gap cues than WTs.
Marble Burying	Pattern of increased marble burying in the TS2-neo mice as indicative of repeat and repetitive behaviors. (Silverman et al. 2010)	TS2-neo mice buried significantly more marbles than WT controls.
Social Dominance Tube Test	TS2-neo mice will show abnormal aggressive behaviors in competitions for territory. (Kazdoba et al. 2016)	TS2-neo mice "won" significantly more competitions for space.
Ultrasonic Vocalizations	Decreased ultrasonic vocalizations from male TS2-neo mice. (Silverman et al. 2010)	TS2-neo mice vocalized significantly *less* after the initial two minutes of the male-female mating interaction.
Morris Water Maze	No deficits in TS2-neo performance. (Bader et al. 2011; Silverman et al. 2010)	No significant differences between Genotype reported, TS2-neo mice learned at the same ability as WTs.
4/8 Radial Arm Maze	We expect we may see deficits in TS2-neo performance on this more difficult cognitive paradigm. (Rendall, Truong, & Fitch 2016)	No significant differences between Genotype reported, TS2-neo mice learned at the same ability as WTs.

Table 2: Summary of predictions for TS2-neo performance and reported results for seven behavioral tasks discussed in *Part 1: Behavioral Phenotyping*

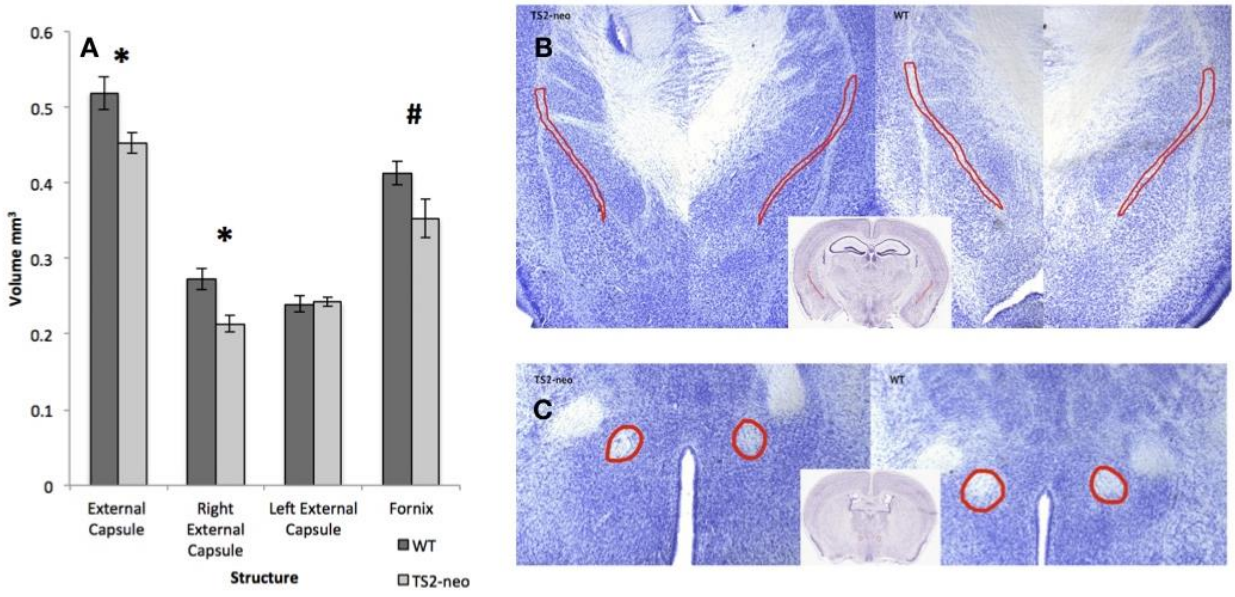

Figure 2: TS2-neo mice show significant decreases in volumes of external capsule, specifically right external capsule, and marginal decrease in the fornix (A) (* $p<.05$, # $p=.059$); location and size of external capsule (outlined in red) compared between representative TS2-neo and WT samples (B); location and size of fornix (outlined in red) compared between representative TS2-neo and WT samples (C).

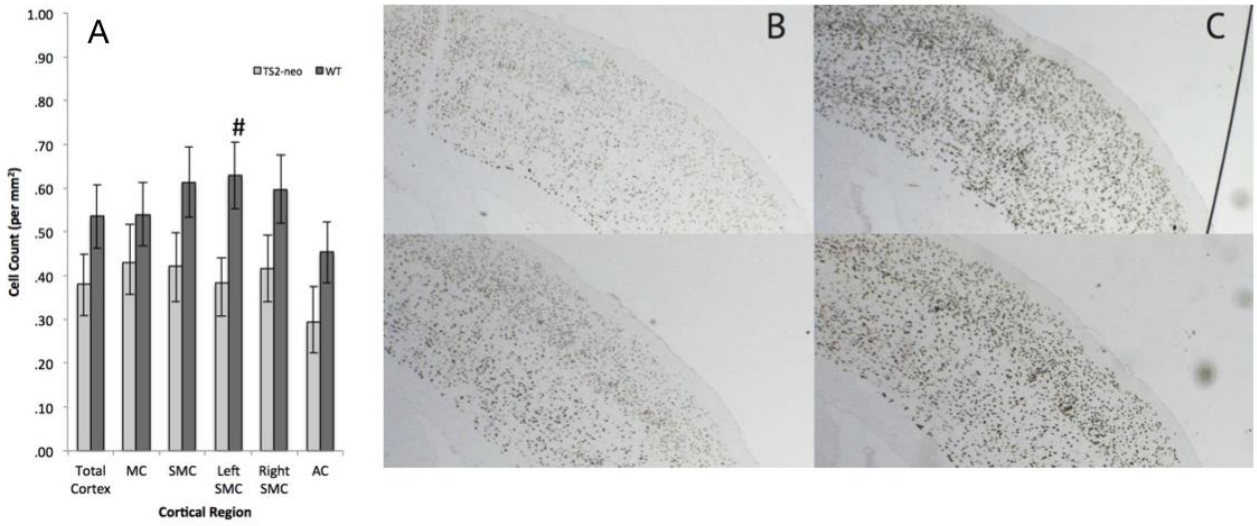

Figure 3: Left somatosensory cortex in TS2-neo knock-in trends towards a significant decrease in *Satb2* expressing callosal projecting neurons, pattern reflected through all cortical regions (# p<.1); (A) (MC - motor cortex, SMC - somatosensory cortex, AC - auditory cortex), n=8 (4 TS2-neo, 4 WT); images of representative TS2-neo (B column) and WT (C column) tissue samples.

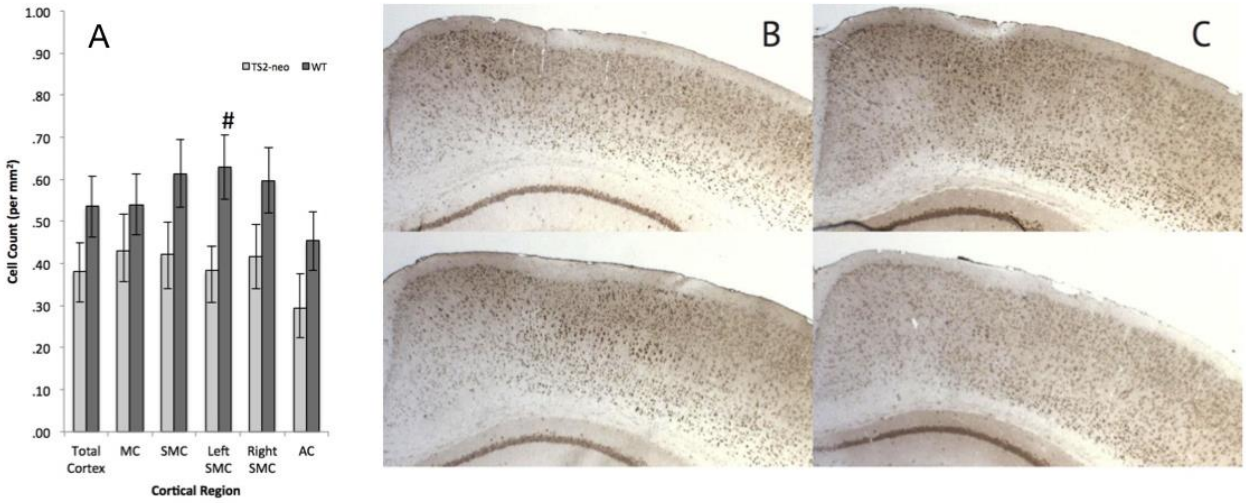

Figure 4: Left motor cortex in TS2-neo knock-in trends towards a significant increase in *Foxp2* expressing deep layer cortical neurons (# $p<.1$); (A), n=8 (4 TS2-neo, 4 WT); images of representative TS2-neo (B column) and WT (C column) tissue samples.

Bregma Level		Right Hemisphere	Left Hemisphere	Average
1.10	Upper Layers	F (1,16) = 2.073 p = .172	F (1,16) = 17.453 p = .001	F(1,16) = 17.371 p = .001
	Deep Layers	F (1,16) = .378 p = . 548	F (1,16) = .096 p = .762	F(1,16) = .287 p = .600
	Total	F (1,16) = .170 p = .686	F (1,16) = 3.798 p = .072	F(1,16) = 2.055 p = .174
.14	Upper Layers	F(1,16) = 3.541 p = .081	F(1,16) = 10.565 p = .006	F(1,16) = 17.371 p = .001
	Deep Layers	F(1,16) = .509 p = .487	F(1,16) = .535 p = .447	F(1,16) = .287 p = .600
	Total Cortex	F(1,16) = .003 p = .954	F(1,16) = .727 p = .408	F(1,16) = 2.055 p = .174
-.94	Upper Layers	F(1,16) = .851 p = .372	F(1,16) = 5.195 p = .039	F(1,16) = 3.081 p = .101
	Deep Layers	F(1,16) = 5.488 p = . 034	F(1,16) = 2.252 p = .156	F(1,16) = 5.001 p = .042
	Total Cortex	F(1,16) = 3.105 p = .100	F(1,16) = .101 p = .921	F(1,16) = .471 p = .504

Table 3: TS2-neo mice show significant increases in the thickness of deep layers (layers 5 and 6 of the motor cortex), in particular the right hemisphere, and significant decreases of upper layer thickness (layers 2-4) in the left hemisphere ($p<.05$).

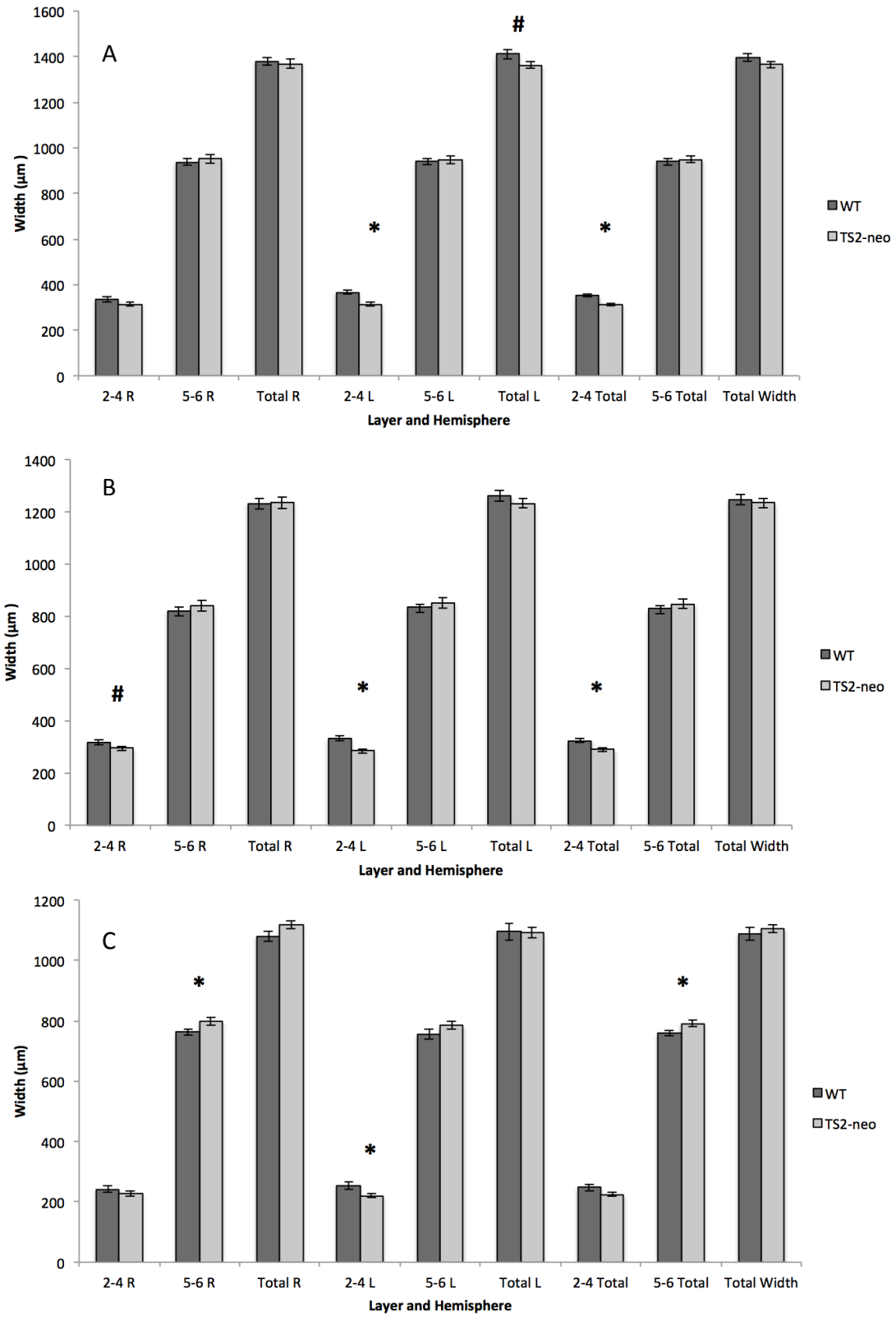

Figure 5: Corresponding plots to Table 3 at bregma levels 1.10, (* p<.05, # p<.1); (A), .14 (B), and -.94 (C)

References

Alexander AL, Lee JE, Lazar M, Boudos R, DuBray MB, Oakes TR*, et al.* Diffusion tensor imaging of the corpus callosum in Autism. Neuroimage 2007, 34: 61–73.

Amaral, D., Schumann, C., & Nordahl, C. (2008). Neuroanatomy Of Autism. *Trends in Neurosciences,31*(3), 137-145. doi:10.1016/j.tins.2007.12.005

Ameis, S., & Catani, M. (2015). Altered white matter connectivity as a neural substrate for social impairment in Autism Spectrum Disorder. *Cortex,* 158-181. doi:doi:10.1016/j.cortex.2014.10.014

American Psychiatric Association. (2013). Diagnostic and statistical manual of mental disorders (5th ed.). Washington, DC: Author.

Bader, P. et al. (2011). Mouse model of Timothy syndrome recapitulates triad of autistic traits. *Proceedings of the National Academy of Sciences, 108*(37), 15432-15437.

Bett, G., Lis, A., Wersinger, S., Baizer, J., Duffey, M., & Rasmusson, R. (2012). A Mouse Model of Timothy Syndrome: A Complex Autistic Disorder Resulting from a Point Mutation in Cav1.2. *North American Journal of Medical Sciences, 5*(3), 135-135

Billeci, L., Calderoni, S., Tosetti, M., Catani, M., & Muratori, F. (2012). White matter connectivity in children with autism spectrum disorders: A tract-based spatial statistics study. *BioMedCentral Neurology*. doi:10.1186/1471-2377-12-148

Britanova, O., Romero, C. D., Cheung, A., Kwan, K. Y., Schwark, M., Gyorgy, A., . . . Tarabykin, V. (2008). Satb2 Is a Postmitotic Determinant for Upper-Layer Neuron Specification in the Neocortex. *Neuron, 57*(3), 378-392. doi:10.1016/j.neuron.2007.12.028

Gomes, E., Rotta, N. T., Pedroso, F. S., Sleifer, P., & Danesi, M. C. (2004). Auditory hypersensitivity in children and teenagers with autistic spectrum disorder. *Arquivos de Neuro-Psiquiatria, 62*(3b), 797-801. doi:10.1590/s0004-282x2004000500011

Ellegood J., Anagnostou E., Babineau B. A., Crawley J. N., Lin L., Genestine M., et al. . (2015). Clustering autism: using neuroanatomical differences in 26 mouse models to gain insight into the heterogeneity. Mol. Psychiatry 20, 118–125. 10.1038/mp.2014.98

Ellegood, J., Babineau, B. A., Henkelman, R. M., Lerch, J. P., & Crawley, J. N. (2013). Neuroanatomical analysis of the BTBR mouse model of autism using magnetic resonance imaging and diffusion tensor imaging. *NeuroImage*, *70*, 288–300. http://doi.org/10.1016/j.neuroimage.2012.12.029

Eigsti, I. M., & Fein, D. A. (2013). More is less: pitch discrimination and language delays in children with optimal outcomes from autism. Autism Research, 6(6), 605-613.

Fitch, R. H., Threlkeld, S. W., McClure, M. M., & Peiffer, A. M. (2008). Use of a modified prepulse inhibition paradigm to assess complex auditory discrimination in rodents. *Brain Research Bulletin*, *76*(0), 1–7. http://doi.org/10.1016/j.brainresbull.2007.07.013

Henry KR, Chole RA. Genotypic differences in behavioral, physiological and anatomical expressions of age-related hearing loss in the laboratory mouse. Audiol. 5:369–383, 1980.

Hyde, L. A., Hoplight, B. J., & Denenberg, V. H. (1998). Water version of the radial-arm maze: learning in three inbred strains of mice. Brain research, 785(2), 236-244.

Jiang, Y., Yuen, R. K. C., Jin, X., Wang, M., Chen, N., Wu, X., … Scherer, S. W. (2013). Detection of Clinically Relevant Genetic Variants in Autism Spectrum Disorder by Whole-Genome Sequencing. *American Journal of Human Genetics*, *93*(2), 249–263. http://doi.org/10.1016/j.ajhg.2013.06.012

Krey, J., Paşca, S., Shcheglovitov, A., Yazawa, M., Schwemberger, R., Rasmusson, R., & Dolmetsch, R. (2013). Timothy syndrome is associated with activity-dependent dendritic retraction in rodent and human neurons. *Nature Neuroscience, 16*(2), 201-209. Retrieved November 3, 2015, from PubMed.

Kwan, K. Y. (2013). Transcriptional dysregulation of neocortical circuit assembly in ASD. *International Review of Neurobiology*, *113*, 167–205. http://doi.org/10.1016/B978-0-12-418700-9.00006-X

Lein, E.S. et al. (2007) Genome-wide atlas of gene expression in the adult mouse brain, Nature 445: 168-176. doi: 10.1038/nature05453

Melillo, R., & Leisman, G. (2009). Autistic Spectrum Disorders as Functional Disconnection Syndrome. *Reviews in the Neurosciences, 20*(2). Retrieved November 3, 2015, from PubMed.

Mostofsky, S., Goldberg, M., Landa, R., & Denckla, M. (2000). Evidence for a deficit in procedural learning in children and adolescents with autism: Implications for cerebellar contribution. *Journal of the International Neuropsychological Society, 6*, 752-759.

Mostofsky, S. H., Powell, S. K., Simmonds, D. J., Goldberg, M. C., Caffo, B., & Pekar, J. J. (2009). Decreased connectivity and cerebellar activity in autism during motor task performance. *Brain*, *132*(9), 2413–2425. http://doi.org/10.1093/brain/awp088

Mottron, L., Dawson, M., Soulieres, I., Hubert, B., & Burack, J. (2006). Enhanced perceptual functioning in autism: An update, and eight principles of autistic perception. Journal of autism and developmental disorders, 36(1), 27-43.

Moy, S. S., Nadler, J. J., Young, N. B., Perez, A., Holloway, L. P., Barbaro, R. P., … Crawley, J. N. (2007). Mouse Behavioral Tasks Relevant to Autism: Phenotypes of Ten Inbred Strains. *Behavioural Brain Research*, *176*(1), 4–20. http://doi.org/10.1016/j.bbr.2006.07.030

Navedo, M., Cheng, E., Yuan, C., Votaw, S., Molkentin, J., Scott, J., & Santana, L. (2010). Increased Coupled Gating of L-Type Ca2 Channels During Hypertension and Timothy Syndrome. *Circulation Research,* 748-756.

Paşca, S., Portmann, T., Voineagu, I., Yazawa, M., Shcheglovitov, A., Paşca, A., et al. (2011). Using iPSC-derived neurons to uncover cellular phenotypes associated with Timothy syndrome. *Nature Medicine,* 1657-1662. doi:10.1038/nm.2576.

Poustka, L., Jennen-Steinmetz, C., Henze, R., & Stieltjes, B. (2012). Fronto-temporal disconnectivity and symptom severity in autism spectrum disorders. *The World Journal of Biological Psychiatry, 13*, 269-280. doi:10.1016/s0924-9338(11)73542-8

Rendall, A. R., Truong, D. T., & Fitch, R. H. (2016). Learning Delays in a mouse model of Autism Spectrum Disorder. *Behavioural Brain Research*, *303*, 201–207. http://doi.org/10.1016/j.bbr.2016.02.006

Scattoni, M. L., Gandhy, S. U., Ricceri, L., & Crawley, J. N. (2008). Unusual Repertoire of Vocalizations in the BTBR T tf/J Mouse Model of Autism. *PLoS One, 3*(8), 1-15. doi:10.1371/journal.pone.0003067

Splawski, I., Timothy, K., Sharpe, L., Decher, N., Kumar, P., Bloise, R., . . . Keating, M. (2004). CaV1.2 Calcium Channel Dysfunction Causes a Multisystem Disorder Including Arrhythmia and Autism. Cell,19-31. doi:10.1016/j.cell.2004.09.011

Truong, D. T., Rendall, A. R., Castelluccio, B. C., Eigsti, I. M., & Fitch, R. H. (2015). Auditory processing and morphological anomalies in medial geniculate nucleus of Cntnap2 mutant mice. Behavioral neuroscience, 129(6), 731.